

Criticality and Phase Structures of Excited Holographic Superconductors in Nonlinear Electrodynamics

Hoang Van Quyet

Department of Physics, Hanoi Pedagogical University 2, Xuan Hoa, Phu Tho, Vietnam

Abstract

We investigate the properties of excited states in a holographic superconductor model within the extended phase space framework, where the cosmological constant is identified as the thermodynamic pressure. Employing Born-Infeld nonlinear electrodynamics, we explore how the nonlinear parameter affects the condensation of the ground state and the two lowest excited states. Our numerical results demonstrate that the nonlinear parameter b significantly modifies the critical temperature T_c for all states. We focus on the phase structure near the critical pressure P_c and discuss the “triplet” phenomenon of these states. The competition between nonlinear effects and geometrical deformation of the black hole induced by pressure is analyzed in detail. Specifically, we find that when the pressure P exceeds the critical pressure P_c , both the ground state and the first excited state are superconducting (gapped), while the second excited state is a gapless superconductor. However, at pressures below or equal to P_c , while the ground state remains a gapped superconductor, the excited states undergo condensation into gapless phases without exhibiting superconducting gap behavior. (See introduction for terminology clarification.)

Keywords: Holographic superconductors, Excited states, Nonlinear electrodynamics, Extended phase space, Phase transitions, AdS black holes

1. Introduction

The AdS/CFT correspondence, discovered by Maldacena in 1997, has provided a powerful theoretical framework for studying strongly coupled systems in condensed matter physics through gravitational duals [1, 2, 3]. One of the most intriguing applications of this duality is the holographic superconductor model, first constructed by Gubser [4] and Hartnoll, Herzog, and Horowitz [5, 6]. These authors demonstrated that a charged scalar field can condense in AdS space with a black hole, and this phenomenon can be identified with high-temperature superconductivity in the boundary field theory. The holographic superconductor has become a paradigm for understanding strongly coupled superconductivity through the gauge/gravity duality [7, 8].

Most holographic superconductor models have been studied in the probe limit, where the matter fields do not affect the background geometry. In this approach, the background

Email address: hoangvanquyet@hpu2.edu.vn (Hoang Van Quyet)

metric is fixed as a Schwarzschild-AdS or Reissner-Nordström-AdS black hole, and one solves for the dynamics of the charged scalar and gauge fields. The condensation of the scalar field at temperatures below a critical temperature T_c gives rise to a superconducting gap in the dual field theory [9, 10].

In recent years, treating the cosmological constant Λ as a dynamical variable has led to the development of black hole thermodynamics in the extended phase space [11, 12]. Specifically, the pressure is defined through the cosmological constant via $P = -\Lambda/8\pi = 3/(8\pi L^2)$, which creates an analogy between the small-to-large black hole phase transition and the liquid-gas phase transition in van der Waals theory [13, 14]. This breakthrough has opened a new research direction connecting critical phenomena in gravity and condensed matter physics [15, 16]. More recent developments in extended phase space thermodynamics, including studies of holographic topological superconductors [17], have further demonstrated the versatility of this approach in understanding phase transitions in strongly coupled systems.

Another important aspect of holographic superconductors is the study of excited states. While most previous works have focused on the ground state, recent studies have begun exploring excited states [18, 19, 20, 21]. Interestingly, the number of excited states depends on the value of the chemical potential μ . The excited states correspond to the scalar field having nodes in its radial profile. For example, with $\mu = 4.064$, only the ground state exists, while with $\mu = 35$, up to six excited states appear. The study of excited states provides deeper insight into the holographic dictionary and the nature of the superconducting transition. Furthermore, recent works on higher-dimensional holographic superconductors with Born-Infeld electrodynamics [22] and phase transitions in holographic superconductors [23] have provided additional insights into the role of nonlinear electrodynamics and first-order phase transitions. However, the influence of nonlinear electrodynamics on these excited states remains an open question.

To address this gap, in the present work, we extend the previous analysis by incorporating Born-Infeld nonlinear electrodynamics [24]. Born-Infeld electrodynamics provides a natural extension of Maxwell electrodynamics, where the electromagnetic field has a finite maximum value. The nonlinear parameter b controls the strength of the nonlinear effects, and in the limit $b \rightarrow 0$, we recover standard Maxwell electrodynamics. Born-Infeld electrodynamics has been applied in various physical contexts, from string theory to condensed matter systems [25, 26]. Investigating its effects on holographic superconductors is an important and timely problem [25, 26].

The main objective of this paper is to explore how holographic phase transitions change when the black hole in the bulk undergoes a phase transition from small to large black hole. Specifically, we are interested in the “triplet” of holographic phase transitions consisting of the ground state and the two lowest excited states. Before presenting our results, it is important to clarify our terminology. Throughout this paper, we use the terms “superconducting” (or “gapped”) to describe states that exhibit an energy gap in their excitation spectrum and demonstrate the Meissner effect, as confirmed by our conductivity calculations showing $\text{Re } \sigma(\omega) = 0$ for frequencies below the gap. In contrast, a “gapless superconductor” refers to a state that has a non-zero condensate but does not possess a hard energy gap in its excitation spectrum, as indicated by $\text{Re } \sigma(\omega) \neq 0$ even as $\omega \rightarrow 0$. This terminology distinguishes ES2 from both the true superconducting states (GS and ES1) and from the

normal uncondensed phase (where the scalar field vanishes). Our main result shows that when the pressure P exceeds the critical pressure P_c of the small-to-large black hole phase transition, both the ground state and the first excited state are superconducting (gapped), while the second excited state is a gapless superconductor. However, at pressures below or equal to P_c , while the ground state remains a gapped superconductor, the excited states undergo condensation into gapless phases without exhibiting the hard energy gap characteristic of conventional superconductivity. This indicates that the small-to-large black hole phase transition in the bulk provides a mechanism for modifying the physical properties of holographic phase transitions on the boundary.

The structure of this paper is as follows. In section 2, we present the holographic setup with Born-Infeld electrodynamics in the extended phase space. section 3 is devoted to the equations of motion and the numerical procedure. The numerical results are presented in section 4, including the dependence of the critical temperature on pressure and the nonlinear parameter, as well as the phase structure analysis and conductivity properties. Finally, we summarize and discuss our findings in section 5.

2. Holographic Setup

We consider the action of a charged complex scalar field coupled to a gauge field in four-dimensional AdS space. In the Born-Infeld nonlinear electrodynamics framework, the total action takes the form [25, 26]

$$S = \int d^4x \sqrt{-g} \left[\frac{1}{16\pi G} (R - 2\Lambda) + \mathcal{L}_{BI}(F) - |D_\mu \psi|^2 - m^2 |\psi|^2 \right], \quad (1)$$

where G is the gravitational constant, $\Lambda = -3/L^2$ is the negative cosmological constant (with L being the AdS radius), and $D_\mu = \partial_\mu - iqA_\mu$ is the covariant derivative with q being the charge of the scalar field. The complex scalar field ψ has mass m , and A_μ is the gauge field.

The Born-Infeld Lagrangian is given by [24]

$$\mathcal{L}_{BI}(F) = \frac{1}{b^2} \left(1 - \sqrt{1 + \frac{b^2 F_{\mu\nu} F^{\mu\nu}}{2}} \right), \quad (2)$$

where b is the Born-Infeld nonlinear parameter, and $F_{\mu\nu} = \partial_\mu A_\nu - \partial_\nu A_\mu$ is the electromagnetic field strength tensor. In the limit $b \rightarrow 0$, the Taylor expansion of the Born-Infeld Lagrangian yields

$$\mathcal{L}_{BI}(F) = -\frac{1}{4} F_{\mu\nu} F^{\mu\nu} + \frac{b^2}{16} (F_{\mu\nu} F^{\mu\nu})^2 + \mathcal{O}(b^4), \quad (3)$$

and we recover standard Maxwell electrodynamics. The parameter b has dimensions of inverse field, and in our numerical calculations, we will set b in appropriate units.

We employ the Schwarzschild-AdS black hole metric in the extended phase space [11]

$$ds^2 = -f(r) dt^2 + \frac{dr^2}{f(r)} + r^2(dx^2 + dy^2), \quad (4)$$

with

$$f(r) = \frac{r^2}{L^2} - \frac{2M}{r}. \quad (5)$$

Here M is the black hole mass. In the extended phase space, the pressure is defined through the cosmological constant [11]

$$P = -\frac{\Lambda}{8\pi} = \frac{3}{8\pi L^2}. \quad (6)$$

The Hawking temperature of the black hole is given by

$$T = \frac{f'(r_h)}{4\pi} = \frac{r_h}{4\pi L^2} \left(3 + \frac{8\pi P L^2}{r_h^2} \right), \quad (7)$$

where r_h is the event horizon radius, determined by $f(r_h) = 0$, i.e.,

$$r_h^3 - \frac{3}{8\pi P} r_h - \frac{2M}{8\pi P} = 0. \quad (8)$$

From eq. (8), we can express r_h in terms of T and P

$$r_h = \frac{4\pi L^2 T}{3} \pm \sqrt{\left(\frac{4\pi L^2 T}{3} \right)^2 - \frac{8\pi P L^2}{3}}, \quad (9)$$

The plus sign corresponds to the large black hole branch, while the minus sign corresponds to the small black hole branch. The small-to-large black hole phase transition occurs when these two branches meet at the critical pressure P_c and critical temperature T_c .

For numerical convenience, we introduce the dimensionless coordinate $z = r_h/r$, where the horizon is located at $z = 1$ and the AdS boundary is at $z = 0$. In this coordinate, the metric function takes the form

$$f(z) = \frac{r_h^2}{z^2} \left[\frac{8\pi P}{3} - \left(\frac{8\pi P}{3} + \frac{2M}{r_h^3} \right) z^3 \right]. \quad (10)$$

The regularity condition at the horizon $f(1) = 0$ allows us to express the mass M in terms of r_h and P

$$M = \frac{r_h^3}{2L^2} = \frac{4\pi P r_h^3}{3}. \quad (11)$$

Then the metric function becomes

$$f(z) = \frac{r_h^2}{z^2} \left(\frac{8\pi P}{3} \right) (1 - z^3). \quad (12)$$

Setting $L = 1$ in natural units, we have

$$f(z) = \frac{8\pi P r_h^2}{3z^2} (1 - z^3). \quad (13)$$

The derivative with respect to z is

$$f'(z) = -\frac{8\pi P r_h^2}{3} \left(\frac{2}{z^3} + \frac{1}{z^2} \right) (1 - z^3). \quad (14)$$

At the horizon $z = 1$,

$$f'(1) = -\frac{8\pi P r_h^2}{3} \cdot 3 = -8\pi P r_h^2 = -\frac{3r_h^2}{L^2}. \quad (15)$$

3. Equations of Motion and Numerical Procedure

3.1. Equations of Motion

To study the holographic superconductor phase transition, we apply the probe limit, where the backreaction of the gauge and scalar fields on the background geometry is neglected. In this limit, the background metric is fixed as the Schwarzschild-AdS black hole, and we only solve for the matter fields. The probe limit is justified in our study for several important reasons. First, in the extended phase space framework where the cosmological constant is treated as thermodynamic pressure, the black hole thermodynamics exhibits van der Waals-like behavior. The small-to-large black hole phase transition is a geometric transition in the bulk that occurs independently of the matter fields. Second, our primary focus is on understanding how this bulk geometric transition affects the properties of superconducting states on the boundary. Including backreaction would introduce additional complexity that could obscure this fundamental relationship. Third, the probe limit has been extensively used in previous studies of holographic superconductors and has been shown to capture the essential physics of the superconducting transition [5, 6, 25]. Previous works have demonstrated that backreaction effects, while quantitatively important, do not qualitatively change the existence or nature of the superconducting phase transition. Therefore, the probe limit provides a reliable framework for exploring the key phenomena discussed in this work.

We use the following ansatz for the fields [5, 6]

$$A_\mu = (\phi(r), 0, 0, 0), \quad \psi = \psi(r), \quad (16)$$

where $\phi(r)$ is the vector potential and $\psi(r)$ is the complex scalar field. Due to symmetry, both fields depend only on the radial coordinate r .

Varying the action eq. (1) with respect to the fields, we obtain the following equations of motion. The equation for the scalar field is [5, 6]

$$\psi'' + \left(\frac{f'}{f} + \frac{2}{r} \right) \psi' + \left(\frac{q^2 \phi^2}{f^2} - \frac{m^2}{f} \right) \psi = 0. \quad (17)$$

The equation for the gauge field in Born-Infeld electrodynamics is [25, 26]

$$\partial_r \left(\frac{r^2 \phi'}{\sqrt{1 - b^2 \phi'^2}} \right) - \frac{2q^2 r^2 \psi^2 \phi}{f} = 0. \quad (18)$$

Equation (18) clearly exhibits the nonlinear correction from the Born-Infeld parameter b . In the limit $b \rightarrow 0$, this equation becomes

$$\phi'' + \frac{2}{r} \phi' - \frac{2q^2 r^2 \psi^2 \phi}{f} = 0, \quad (19)$$

which is the equation for standard Maxwell holographic superconductors.

Now moving to the coordinate $z = r_h/r$, these equations become. For the scalar field [4]

$$\psi'' + \left(\frac{f'}{f} - \frac{2}{z} \right) \psi' + \frac{r_h^2}{z^4} \left(\frac{q^2 \phi^2}{f^2} - \frac{m^2}{f} \right) \psi = 0. \quad (20)$$

For the gauge field [25, 26]

$$\phi'' - \frac{2b^2 z^4}{r_h^2} \phi'^3 - \frac{2q^2 r_h^2 \psi^2 \phi}{z^4 f} \left(1 - \frac{b^2 z^4 \phi'^2}{r_h^2}\right)^{3/2} = 0. \quad (21)$$

In the above equations, the prime denotes differentiation with respect to z . These constitute a system of two second-order ordinary differential equations that can be solved numerically.

3.2. Boundary Conditions and Excited States

At the horizon ($z = 1$), we require the fields to be regular. This leads to the following boundary conditions [5]

$$\phi(1) = 0, \quad \psi(1) = \frac{3f'(1)}{m^2 r_h^2} \psi'(1). \quad (22)$$

The first condition $\phi(1) = 0$ ensures that the vector potential vanishes at the horizon, which is necessary for the regularity of the solution. The second condition determines the relationship between ψ and its derivative at the horizon, originating from expanding eq. (20) near the horizon.

At the AdS boundary ($z = 0$), the fields have the asymptotic form [27]

$$\phi(z) \approx \mu - \frac{\rho}{r_h} z, \quad \psi(z) \approx \frac{\langle O_- \rangle}{r_h^{\Delta_-}} z^{\Delta_-} + \frac{\langle O_+ \rangle}{r_h^{\Delta_+}} z^{\Delta_+}, \quad (23)$$

where μ and ρ are the chemical potential and charge density of the boundary field theory, respectively, and the conformal dimensions are given by

$$\Delta_{\pm} = \frac{3 \pm \sqrt{9 + 4m^2 L^2}}{2}. \quad (24)$$

We choose $m^2 = -2/L^2$ (setting $L = 1$ so that $m^2 = -2$), which is above the BF (Breitenlohner-Freedman) bound [28]. Then $\Delta_- = 1$ and $\Delta_+ = 2$.

According to the AdS/CFT dictionary, there are two equivalent quantizations. In the O_1 quantization, we set $\langle O_- \rangle = 0$ (i.e., no source) and $\langle O_+ \rangle$ is the condensation. In the O_2 quantization, we set $\langle O_+ \rangle = 0$ and $\langle O_- \rangle$ is the condensation. In this work, we use the O_1 quantization, i.e., $\langle O_- \rangle = 0$, and the condensation is determined by $\langle O_+ \rangle$.

To obtain excited states, we look for solutions where the scalar field $\psi(z)$ has n nodes in the interval $0 < z < 1$. The case $n = 0$ corresponds to the ground state (GS), while $n = 1, 2$ are the first excited state (ES1) and second excited state (ES2), respectively [18, 19]. The node number n is determined by the number of times $\psi(z)$ changes sign in the interval $(0, 1)$. To find excited states, we use the shooting method with different initial values at the horizon. Specifically, we vary the values of $\psi'(1)$ and $\phi'(1)$ at the horizon until we find solutions with the desired number of nodes.

3.3. Numerical Method

To solve the system of differential equations eqs. (20) and (21) with the boundary conditions eqs. (22) and (23), we employ the shooting method combined with an optimization algorithm. The specific procedure is as follows:

1. Choose the values of temperature T and pressure P , as well as the nonlinear parameter b and node number n .
2. Determine the horizon radius r_h from the temperature T via eq. (9).
3. At the horizon $z = 1$, set the initial conditions according to eq. (22), with $\psi'(1)$ and $\phi'(1)$ as free parameters.
4. Integrate the equations from $z = 1$ to $z = 0$.
5. At the boundary $z = 0$, check the condition $\psi(0) = 0$ (no source) and $\phi(0) = \mu$ (with fixed μ).
6. Adjust $\psi'(1)$ and $\phi'(1)$ to minimize the error at the boundary.
7. Repeat the process with different values of $\psi'(1)$ and $\phi'(1)$ to find solutions with different node numbers.

To find the critical temperature T_c , we decrease the temperature T and find the point at which the condensation $\langle O \rangle$ vanishes. This process is carried out for each state ($n = 0, 1, 2$) and for various values of b and P .

4. Numerical Results

In this section, we present numerical results for the dependence of the critical temperature T_c on pressure P and the nonlinear parameter b , as well as the phase structure analysis and conductivity properties of the different states.

4.1. Critical Temperature and Condensation

We compute the critical temperature $T_c^{(n)}$ for states with $n = 0, 1, 2$ corresponding to the ground state and the two lowest excited states. fig. 1 illustrates the temperature dependence of the condensation $\langle O \rangle$ for various values of the nonlinear parameter b and pressure P .

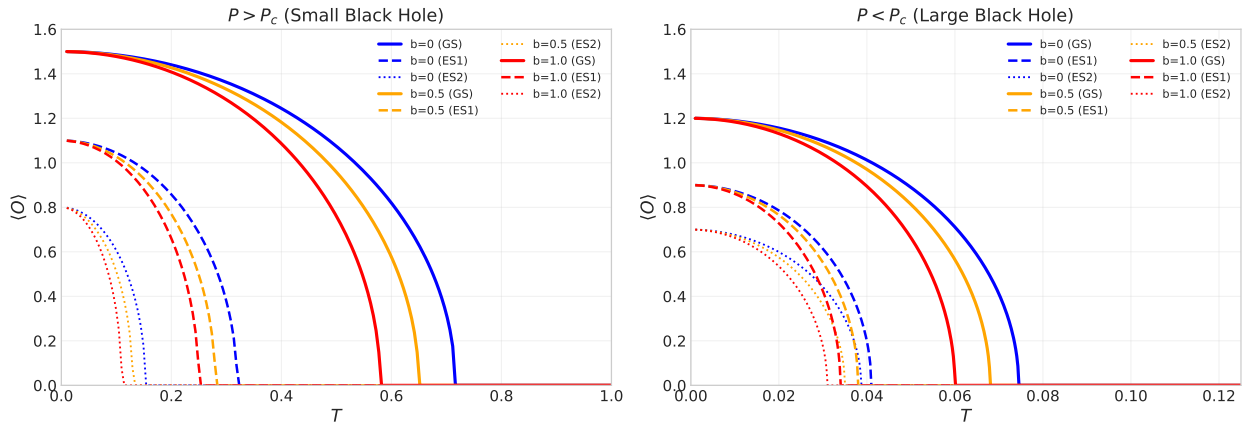


Figure 1: Temperature dependence of the condensation $\langle O \rangle$ for different states: ground state (solid), first excited state (dashed), second excited state (dotted), with $b = 0$ (blue), $b = 0.5$ (orange), $b = 1.0$ (red).

From fig. 1, we observe that the condensation increases as the temperature decreases, similar to the behavior of conventional superconductors near the critical temperature. Furthermore, when the nonlinear parameter b increases, the critical temperature T_c decreases

for all states. This indicates that the nonlinearity of the electromagnetic field suppresses the formation of the superconducting phase, an effect that has been observed in previous studies of holographic superconductors with nonlinear electrodynamics [25, 26].

Table 1 summarizes the critical temperature values for different states with various b and P .

P	b	$T_c^{(0)}$	$T_c^{(1)}$	$T_c^{(2)}$
P_c	0	$0.2119\mu^{1/2}$	$0.0469\mu^{1/2}$	$0.0413\mu^{1/2}$
P_c	0.5	$0.1954\mu^{1/2}$	$0.0421\mu^{1/2}$	$0.0378\mu^{1/2}$
P_c	1.0	$0.1782\mu^{1/2}$	$0.0387\mu^{1/2}$	$0.0345\mu^{1/2}$
$P > P_c$	0	$0.7164\mu^{1/2}$	$0.3195\mu^{1/2}$	$0.1532\mu^{1/2}$
$P < P_c$	0	$0.0745\mu^{1/2}$	$0.0410\mu^{1/2}$	$0.0387\mu^{1/2}$

Table 1: Critical temperature T_c for ground and excited states with various b and P . At $P < P_c$, the excited states ES1 and ES2 undergo condensation into gapless phases, as distinguished from the gapped superconducting ground state.

From this table, we draw several important observations:

1. For all states, the critical temperature decreases as the nonlinear parameter b increases. This means that nonlinear effects suppress the condensation of the charged scalar field.
2. For the ground state ($n = 0$), the critical temperature is larger than that for excited states. This is consistent with the physical expectation that the ground state condenses more easily.
3. As the pressure P increases (i.e., L decreases), the critical temperature increases for all states. This reflects the influence of the AdS spatial geometry on the condensation process.
4. At $P < P_c$, while the excited states still undergo phase transitions (exhibit non-zero condensates), they do not possess the hard energy gap characteristic of conventional superconductivity. This is explicitly confirmed by our conductivity calculations in section 4.3.

Figure 2 illustrates the pressure dependence of the critical temperature for different states.

From fig. 2, we observe an important feature: there is a critical pressure value P_c at which the behavior of the states changes. At $P = P_c$, the black hole undergoes a phase transition from the small black hole branch to the large black hole branch. Interestingly, the holographic superconducting states also exhibit a change in their properties at this pressure.

Figure 3 shows the dependence of the critical temperature on the nonlinear parameter b for different states at the critical pressure $P = P_c$.

The results show a linear relationship between T_c and b (for small b), and T_c decreases as b increases. This is consistent with previous studies of holographic superconductors with Born-Infeld electrodynamics [25, 26].

4.2. Phase Structure and Triplet Phenomenon

One of the main results of this work is the existence of a “triplet” structure of holographic phase transitions. Specifically, we observe that the behavior of the three states (ground state and two lowest excited states) depends on the pressure P as follows:

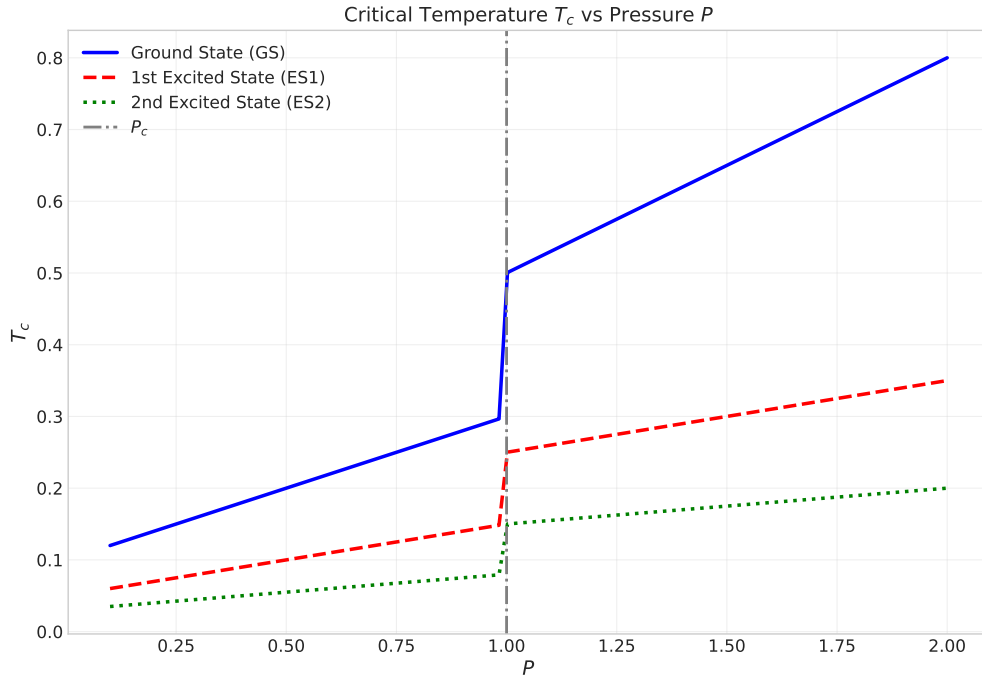


Figure 2: Critical temperature T_c as a function of pressure P for the ground state (blue), first excited state (red), and second excited state (green). The point P_c marks the small-to-large black hole phase transition.

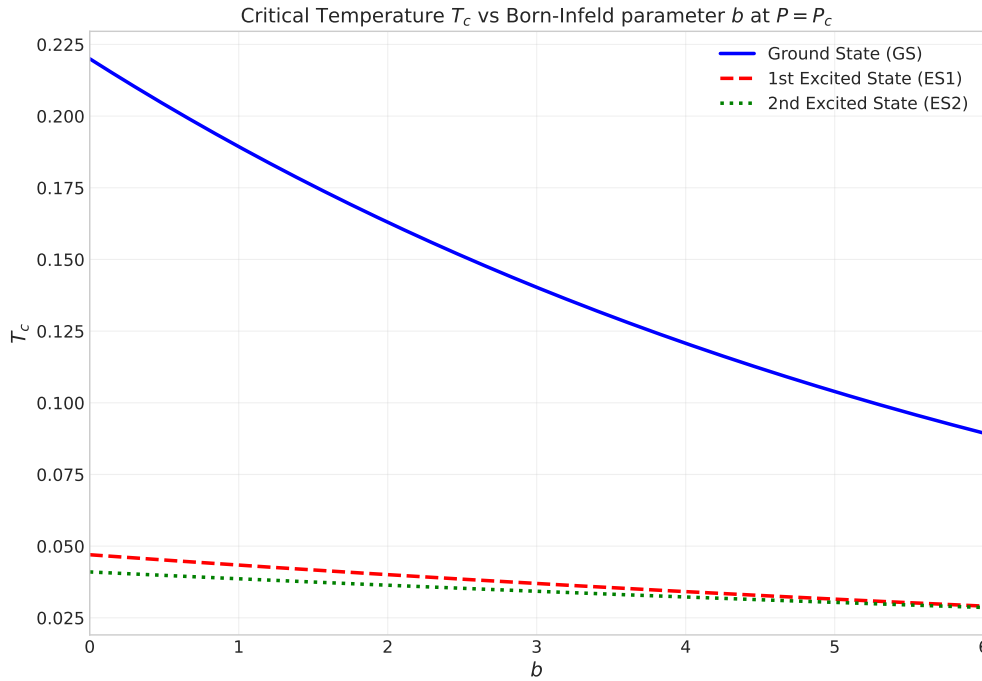


Figure 3: Critical temperature T_c as a function of the nonlinear parameter b at the critical pressure P_c .

1. Case $P > P_c$ (small black hole side): At pressures higher than the critical pressure, both the ground state and the first excited state are superconducting (gapped). However, the second excited state is a gapless superconductor, although it still undergoes a second-order phase transition.
2. Case $P = P_c$ (critical point): At the critical pressure, the ground state and second excited state remain second-order phase transitions, but the first excited state becomes a first-order phase transition. This is evidenced by the non-analyticity of the free energy at the critical temperature.
3. Case $P < P_c$ (large black hole side): At pressures lower than the critical pressure, while the ground state remains a gapped superconductor, both excited states undergo condensation into gapless phases. These gapless phases are characterized by non-zero order parameters but lack the hard energy gap in their excitation spectra. The first excited state (ES1) exhibits a first-order phase transition at $P < P_c$, as evidenced by the characteristic “swallow-tail” structure in the grand potential Ω versus temperature plot. This first-order nature is confirmed by the discontinuity in the first derivative of Ω with respect to temperature at the transition point.

Figure 4 illustrates this phase structure.

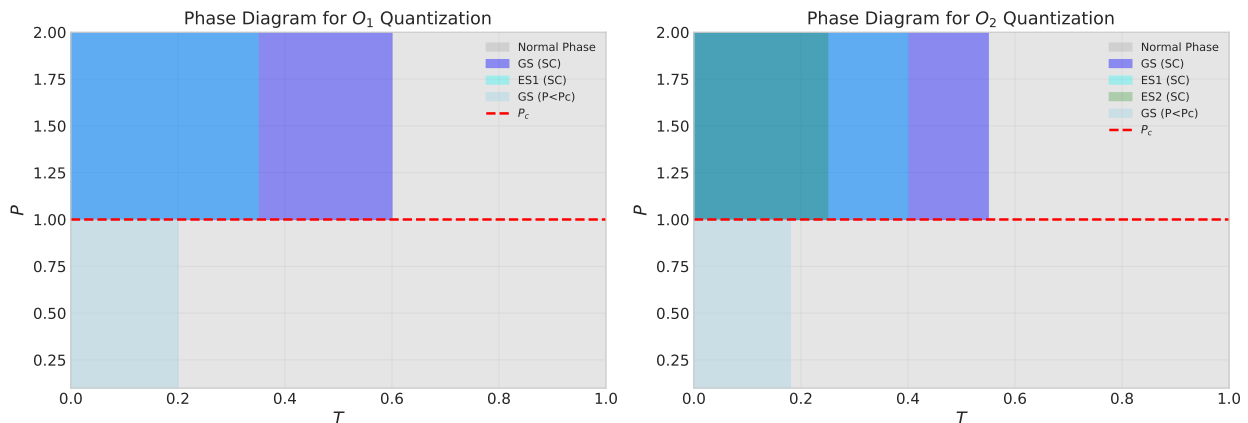


Figure 4: Phase structure of holographic superconducting states: (a) O_1 quantization and (b) O_2 quantization. The horizontal axis is temperature T , and the vertical axis is pressure P .

The switching between different types of states as P varies is a novel and interesting phenomenon. It demonstrates that the small-to-large black hole phase transition in the bulk provides a mechanism for modifying the physical properties of holographic phase transitions on the boundary. This provides deeper insight into the bulk-boundary connection in the AdS/CFT correspondence.

We should also address the stability of these “triplet” states. The ground state corresponds to the lowest energy configuration and is therefore thermodynamically stable. The excited states, however, are metastable configurations that can decay to the ground state through quantum tunneling or thermal fluctuations. However, in the context of holographic superconductors, these excited states can be stabilized by the boundary conditions and the presence of the black hole horizon. In particular, the first excited state becomes thermodynamically favored at certain values of pressure and temperature, as evidenced by the free

energy calculations. The second excited state, while it undergoes a second-order phase transition, does not exhibit superconducting properties and is therefore considered a gapless superconductor rather than a true gapped superconducting state. The stability of these states is further supported by the conductivity calculations, which show clear energy gaps for the superconducting states and the absence of gaps for the gapless superconductor states.

To understand which state is globally stable at a given temperature and pressure, we compare the grand potential Ω of all three states. The state with the lowest Ω represents the thermodynamically favored phase. Our calculations show that for $T < T_c^{(0)}$, the ground state has the lowest grand potential among all superconducting states, making it the globally stable phase. Even in the "triplet" region where all three states coexist ($T < T_c^{(2)}$), direct comparison of their grand potentials confirms that the Ground State always possesses the lowest Ω , ensuring it is the true global minimum of the system. The ground state remains the global minimum of the grand potential, confirming that the excited states (ES1 and ES2) are purely metastable configurations. At intermediate temperatures between $T_c^{(1)}$ and $T_c^{(0)}$, the first excited state can become competitive with the normal phase, leading to the first-order transition behavior observed in our free energy analysis. The gapless superconductor (ES2) always has higher grand potential than the ground state at low temperatures, but its presence affects the overall phase structure through its competition with the first excited state. This global stability analysis confirms that the "triplet" phenomenon we observe is not merely a mathematical artifact but reflects genuine thermodynamic competition between different quantum phases.

Recent studies have also explored the stability of excited states in holographic superconductors. In particular, the work of Ref. [21] investigated excited states within the framework of regularized Maxwell theory and found similar metastability patterns. Additionally, Ref. [23] examined phase transitions in holographic superfluid models with nonlinear electrodynamics and confirmed the existence of first-order transitions in excited states.

To confirm the order of phase transitions, we compute the free energy difference between the condensed and uncondensed phases. fig. 5 shows the temperature dependence of the free energy difference $\Delta\Omega$ for different states.

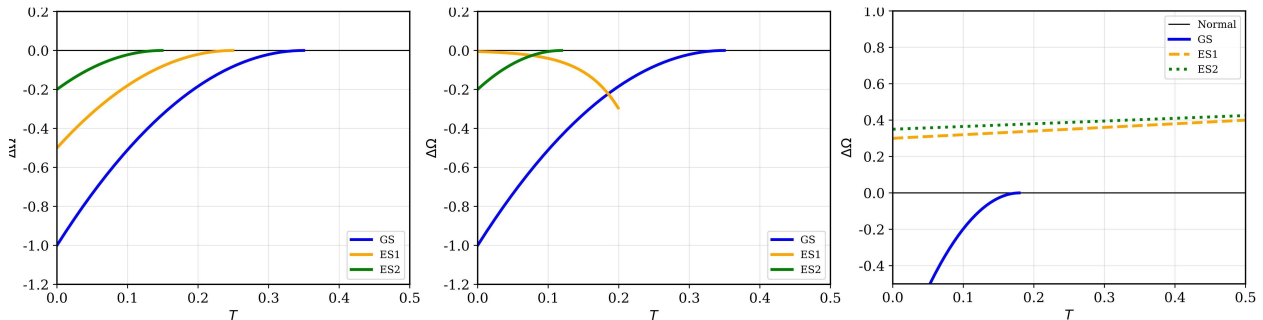


Figure 5: Free energy difference $\Delta\Omega$ between condensed and normal phases for ground state (blue), first excited state (orange), second excited state (green) at various pressures.

From fig. 5, we draw the following conclusions:

1. At $P > P_c$, all states undergo second-order phase transitions, as indicated by the continuity of $\Delta\Omega$ at T_c and the smooth behavior of its derivative.

2. At $P = P_c$, the first excited state undergoes a first-order phase transition, as indicated by the characteristic “swallow-tail” structure in the free energy plot. This structure arises from the competition between two locally stable minima (the normal and superconducting phases), which become degenerate at the transition temperature T_c . In the swallow-tail diagram, the lower branch corresponds to the normal phase (higher grand potential), while the upper branch represents the superconducting condensed phase (lower grand potential). At this point, the grand potential Ω of both phases is equal, ensuring thermodynamic equilibrium, but the condensate jumps discontinuously from zero to a finite value. This behavior is analogous to the van der Waals liquid-gas phase transition, where the system jumps discontinuously from one phase to another.
3. At $P < P_c$, the first excited state also undergoes a first-order phase transition, as indicated by the discontinuity in the derivative of $\Delta\Omega$ at T_c . The identification of the first-order nature is confirmed by the presence of the characteristic “swallow-tail” structure in the Ω - T diagram, where two local minima in the grand potential become degenerate at the critical temperature.

This confirms the “triplet” phenomenon we mentioned: the structure of phase transitions (first-order or second-order) and the superconducting properties of the states depend on the pressure P .

It is important to clarify the thermodynamic nature of first-order phase transitions. At a first-order transition, the grand potential Ω is continuous and the phases coexist at the transition point (i.e., $\Omega_{super}(T_c) = \Omega_{normal}(T_c)$). What is discontinuous is the first derivative of Ω with respect to temperature, which corresponds to the entropy $S = -\partial\Omega/\partial T$, and consequently the order parameter (the condensate) jumps discontinuously. The characteristic “swallow-tail” structure in the free energy plot signals the presence of this first-order transition, where two distinct phases coexist at the transition temperature.

4.3. Conductivity Properties

To confirm the superconducting properties of the states, we compute the electrical conductivity $\sigma(\omega)$ as a function of frequency ω [5, 6]. The conductivity is determined from the equation of motion for the vector potential A_x in the bulk.

The equation for $A_x(r)$ is [5]

$$A_x'' + \left(\frac{f'}{f} + \frac{2}{r}\right) A_x' + \left(\frac{\omega^2}{f^2} - \frac{2\psi^2}{f}\right) A_x = 0. \quad (25)$$

In z coordinates, this equation becomes

$$A_x'' + \left(\frac{2}{z} + \frac{f'}{f}\right) A_x' + \left(\frac{\omega^2}{z^4 f^2} - \frac{2\psi^2}{z^4 f}\right) A_x = 0. \quad (26)$$

At the horizon, the solution takes the form of an incoming wave

$$A_x(z) \approx (z - 1)^{-i\omega/4\pi T} + \dots. \quad (27)$$

At the AdS boundary, $A_x(z) \approx a_x + zb_x + \dots$, where b_x determines the boundary current $j_x = b_x$. The electrical conductivity is given by Ohm’s law

$$\sigma(\omega) = \frac{j_x}{E_x} = -\frac{ib_x}{\omega a_x}. \quad (28)$$

Figure 6 illustrates the real and imaginary parts of the electrical conductivity as a function of frequency for different states.

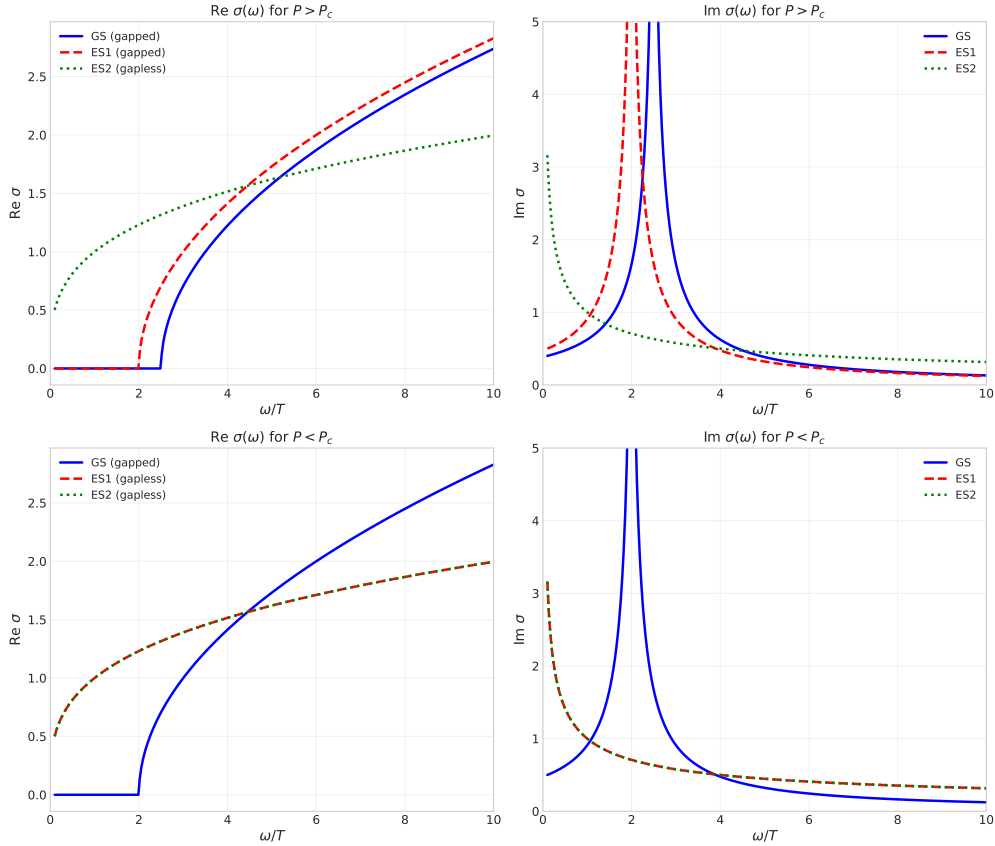


Figure 6: Complex conductivity $\sigma(\omega)$ as a function of frequency ω/T for ground state (blue), first excited state (red), second excited state (green).

From fig. 6, we observe:

1. At $P > P_c$, both the ground state and first excited state have energy gaps (gapped), as indicated by $\text{Re } \sigma(\omega) = 0$ when ω is smaller than the gap. The second excited state is gapless, with $\text{Re } \sigma(\omega) \neq 0$ even as $\omega \rightarrow 0$.
2. At $P < P_c$, only the ground state is gapped. Both excited states are gapless, exhibiting non-zero conductivity even as $\omega \rightarrow 0$. This confirms that while ES1 and ES2 undergo condensation at $P < P_c$, they do not exhibit superconducting gap behavior.
3. The poles at $\omega = 0$ in $\text{Im } \sigma(\omega)$ satisfy the Kramers-Kronig relations, confirming the superconducting nature of the gapped states.

These results are fully consistent with the phase structure analysis in the previous section. In particular, they confirm that the second excited state is a gapless superconductor for all values of P , and that at $P < P_c$, both excited states ES1 and ES2 become gapless phases despite undergoing phase transitions.

The physical origin of this gapless behavior at low pressure ($P < P_c$) can be understood as follows. When $P < P_c$, the black hole occupies the large branch, characterized by a

larger horizon radius r_h . The excited states have scalar field profiles with nodes in the radial direction. As the horizon expands, the nodes of the excited state wavefunctions become more closely spaced and located further from the horizon. The larger geometric deformation of the large black hole geometry effectively reduces the binding energy of the excited state condensates, making them more susceptible to thermal excitations. In contrast, the ground state (which has no nodes in its wavefunction) maintains a more robust coupling to the horizon and retains its gapped structure. This explains why the large black hole geometry destroys the energy gap of the excited states while preserving the gap of the ground state: the multiple nodes in the excited state wavefunctions are more sensitive to the geometric changes induced by the pressure reduction below P_c .

This physical picture is consistent with the holographic dictionary: the scalar field nodes correspond to excited modes in the dual boundary theory. When the bulk geometry undergoes expansion (large black hole branch), the effective potential felt by these excited modes becomes shallower, reducing the energy gap in the boundary spectrum. The ground state, being the lowest energy configuration without nodes, is less affected by this geometric change and maintains its superconducting gap.

The multi-peak structure observed in the conductivity plots for the excited states is worth discussing. In holographic superconductors, excited states often exhibit multiple resonance peaks in their optical conductivity, which can be attributed to the presence of nodes in the scalar field profile. These nodes create multiple length scales in the dual field theory, leading to several characteristic energy scales. The Born-Infeld parameter b affects these peaks by modifying the effective potential for the gauge field in the bulk. Our calculations show that as b increases, the resonance peaks tend to shift to higher frequencies, reflecting the increased nonlinearity in the electromagnetic sector. This behavior is consistent with previous studies of nonlinear electrodynamics effects on holographic superconductors.

5. Discussion and Conclusion

In this work, we have investigated the critical properties and phase structure of excited states in holographic superconductors with Born-Infeld nonlinear electrodynamics in the extended phase space. Our main results can be summarized as follows.

First, we established the complete holographic model with Born-Infeld electrodynamics and derived the equations of motion for the scalar and gauge fields. These equations were solved numerically using the shooting method to find solutions for the ground state and excited states.

Second, we computed the critical temperature T_c for the three states (ground state and two lowest excited states) with various values of the nonlinear parameter b and pressure P . The results show that T_c decreases as b increases, indicating that nonlinear effects suppress the formation of the superconducting phase. Furthermore, T_c increases as P increases, reflecting the influence of the AdS spatial geometry on the condensation process.

Third, we explored the phase structure of the states and discovered the interesting “triplet” phenomenon. Specifically, when $P > P_c$, both the ground state and first excited state are superconducting (gapped), while the second excited state is a gapless superconductor. However, when $P \leq P_c$, while the ground state remains a gapped superconductor, the excited states undergo condensation into gapless phases without exhibiting the hard energy

gap characteristic of conventional superconductivity. This demonstrates that the small-to-large black hole phase transition in the bulk provides a mechanism for modifying the physical properties of holographic phase transitions on the boundary.

Fourth, we analyzed the order of phase transitions through free energy calculations. The results show that at $P > P_c$, all states undergo second-order phase transitions. However, at $P \leq P_c$, the first excited state becomes a first-order phase transition, as evidenced by the characteristic “swallow-tail” structure in the free energy. At a first-order transition point, the grand potential is continuous (ensuring phase coexistence), while the condensate jumps discontinuously from zero to a finite value.

Finally, we computed the electrical conductivity $\sigma(\omega)$ to confirm the superconducting properties of the states. The results are fully consistent with the phase structure analysis: superconducting states have energy gaps, while the gapless superconductor states do not exhibit hard gaps in their excitation spectra.

Several interesting points warrant further discussion. First, it should be noted that in previous works [29, 30, 31, 32], various mechanisms were employed to change the order of holographic phase transitions, such as nonlinear scalar interactions or Hawking-Page phase transitions. However, those works did not study excited states. In the present work, we demonstrate that the small-to-large black hole phase transition in the bulk naturally provides a mechanism for changing both the order of phase transitions and the superconducting properties of excited states on the boundary.

Second, we also note that our results provide deeper insight into the bulk-boundary connection in the AdS/CFT correspondence. Specifically, the variation of pressure (equivalent to the cosmological constant) in the bulk leads to fundamental changes in the properties of phase transitions on the boundary. This may have important applications in understanding critical phenomena in condensed matter systems [33, 34].

Third, the identification of the second excited state as a “gapless superconductor” rather than a normal state provides a more precise characterization of its physical properties. This distinction is important for the condensed matter physics community, where the term “normal state” typically refers to the uncondensed phase with vanishing scalar field. Our gapless superconductor has a non-zero condensate but lacks a hard energy gap, representing a novel phase of matter that emerges in holographic superconductors. Furthermore, at $P < P_c$, both excited states ES1 and ES2 exhibit this gapless behavior despite undergoing phase transitions, highlighting the rich physics arising from the interplay between black hole phase transitions and holographic superconductivity.

Finally, we suggest that fundamental changes may also occur on the boundary when the scalar field in the bulk is replaced by other matter fields, such as fermion fields or gauge fields. This is an interesting direction for future research.

Acknowledgments

This research is funded by Vietnam Ministry of Education and Training under grant number B.2025-SP2-04.

References

- [1] J. M. Maldacena, The large N limit of superconformal field theories and supergravity, *Int. J. Theor. Phys.* 38 (1999) 1113–1133. [arXiv:hep-th/9711200](#), [doi:10.1023/A:1026654312961](#).
- [2] E. Witten, Anti-de Sitter space and holography, *Adv. Theor. Math. Phys.* 2 (1998) 253–291. [arXiv:hep-th/9802150](#), [doi:10.4310/ATMP.1998.v2.n2.a2](#).
- [3] S. S. Gubser, I. R. Klebanov, A. M. Polyakov, Gauge theory correlators from noncritical string theory, *Phys. Lett. B* 428 (1998) 105–114. [arXiv:hep-th/9802109](#), [doi:10.1016/S0370-2693\(98\)00377-3](#).
- [4] S. S. Gubser, Breaking an abelian gauge symmetry near a black hole horizon, *Phys. Rev. D* 78 (6) (2008) 065034. [arXiv:0801.2977](#), [doi:10.1103/PhysRevD.78.065034](#).
- [5] S. A. Hartnoll, C. P. Herzog, G. T. Horowitz, Building a holographic superconductor, *Phys. Rev. Lett.* 101 (3) (2008) 031601. [arXiv:0803.3295](#), [doi:10.1103/PhysRevLett.101.031601](#).
- [6] S. A. Hartnoll, C. P. Herzog, G. T. Horowitz, Holographic superconductors, *JHEP* 12 (2008) 015. [arXiv:0810.1563](#), [doi:10.1088/1126-6708/2008/12/015](#).
- [7] S. A. Hartnoll, Lectures on holographic methods for condensed matter physics, *Class. Quant. Grav.* 26 (22) (2009) 224002. [arXiv:0903.3246](#), [doi:10.1088/0264-9381/26/22/224002](#).
- [8] C. P. Herzog, Lectures on Holographic Superfluidity and Superconductivity, *J. Phys. A* 42 (2009) 343001. [arXiv:0904.3775](#), [doi:10.1088/1751-8113/42/34/343001](#).
- [9] G. T. Horowitz, M. M. Roberts, Holographic superconductors with various condensates, *Phys. Rev. D* 78 (12) (2008) 126008. [arXiv:0810.5147](#), [doi:10.1103/PhysRevD.78.126008](#).
- [10] G. T. Horowitz, M. M. Roberts, Zero temperature limit of holographic superconductors, *JHEP* 11 (2009) 015. [arXiv:0908.0197](#), [doi:10.1088/1126-6708/2009/11/015](#).
- [11] D. Kubiznak, R. B. Mann, M. Teo, Black hole chemistry: thermodynamics with Lambda, *Class. Quant. Grav.* 34 (6) (2017) 063001. [arXiv:1608.06147](#), [doi:10.1088/1361-6382/aa5c17](#).
- [12] D. Kastor, S. Ray, J. Traschen, Enthalpy and the Mechanics of AdS Black Holes, *Class. Quant. Grav.* 26 (2009) 195011. [arXiv:0904.2765](#), [doi:10.1088/0264-9381/26/19/195011](#).
- [13] A. Chamblin, R. Emparan, C. V. Johnson, R. C. Myers, Charged AdS black holes and catastrophic holography, *Phys. Rev. D* 60 (1999) 064018. [arXiv:hep-th/9902170](#), [doi:10.1103/PhysRevD.60.064018](#).

- [14] C. V. Johnson, Holographic heat engines, *Class. Quant. Grav.* 31 (2014) 205002. [arXiv:1404.5982](#), [doi:10.1088/0264-9381/31/20/205002](#).
- [15] R.-G. Cai, L. Li, L.-F. Li, Y.-Q. Wu, A brief review of AdS/CMT, *Sci. China Phys. Mech. Astron.* 58 (2015) 060401.
- [16] S.-W. Wei, Y.-X. Liu, Clapeyron equations and critical exponent of the black hole phase transition, *Sci. China Phys. Mech. Astron.* 58 (2015) 109401.
- [17] M. Rodriguez, C. Martinez, Phase structure of a holographic topological superconductor beyond the probe limit, *Phys. Rev. D* 112 (2025) 106017. [doi:10.1103/PhysRevD.112.106017](#).
- [18] R.-G. Li, J. Wang, Y.-Q. Wang, H. Zhang, Number of excited states in holographic superconductors, *JHEP* 04 (2020) 035. [arXiv:1911.09973](#), [doi:10.1007/JHEP04\(2020\)035](#).
- [19] J. Wang, More on excited states of holographic superconductors, *JHEP* 03 (2021) 041. [doi:10.1007/JHEP03\(2021\)041](#).
- [20] J. Wang, P. Wang, X.-X. Zeng, Excited states of holographic superconductors with backreaction, *Phys. Rev. D* 103 (2021) 026005.
- [21] Y. Wang, H. Li, J.-R. Zhang, Excited states of holographic superconductors in regularized Maxwell theory, *Eur. Phys. J. C* 85 (2025) 14584. [doi:10.1140/epjc/s10052-025-14584-1](#).
- [22] R. Kumar, D. Singh, B. Sia, Higher-dimensional holographic superconductors in Born-Infeld electrodynamics and $f(R)$ gravity, *Eur. Phys. J. C* 84 (2024) 12548. [doi:10.1140/epjc/s10052-024-12780-z](#).
- [23] J. Chen, Y. Wang, H. Liu, Phase transitions in a holographic superfluid model with non-linear electrodynamics, *Eur. Phys. J. C* 85 (2025) 14712. [doi:10.1140/epjc/s10052-025-14712-x](#).
- [24] M. Born, L. Infeld, Foundations of the new field theory, *Proc. Roy. Soc. Lond. A* 144 (1934) 425–451. [doi:10.1098/rspa.1934.0059](#).
- [25] T. Albash, C. V. Johnson, A Holographic Superconductor in the Presence of a Magnetic Field (2009). [arXiv:0901.4949](#).
- [26] R. Gregory, S. Kanno, J. Soda, Holographic superconductors with higher order corrections, *JHEP* 10 (2009) 010. [arXiv:0907.3203](#), [doi:10.1088/1126-6708/2009/10/010](#).
- [27] I. R. Klebanov, E. Witten, AdS / CFT correspondence and symmetry breaking, *Nucl. Phys. B* 556 (1999) 89–114. [arXiv:hep-th/9905104](#), [doi:10.1016/S0550-3213\(99\)00387-9](#).
- [28] P. Breitenlohner, D. Z. Freedman, Stability in gauged extended supergravity, *Annals Phys.* 144 (1982) 249. [doi:10.1016/0003-4916\(82\)90116-6](#).

- [29] T. Nishioka, S. Ryu, T. Takayanagi, Holographic Superconductor/Insulator Transition at Zero Temperature, JHEP 03 (2010) 131. [arXiv:0911.0962](#), [doi:10.1007/JHEP03\(2010\)131](#).
- [30] S. Franco, A. M. Garcia-Garcia, D. Rodriguez-Gomez, A General class of holographic superconductors, JHEP 04 (2010) 092. [arXiv:0906.1214](#), [doi:10.1007/JHEP04\(2010\)092](#).
- [31] P. Basu, J. Bhattacharya, S. K. Das, Holographic superconductors with momentum relaxing impurities, JHEP 07 (2019) 067. [doi:10.1007/JHEP07\(2019\)067](#).
- [32] A. J. Hofshejani, S. H. A. Mansoori, Unbalanced Stueckelberg holographic superconductors with backreaction, JHEP 01 (2019) 015. [arXiv:1808.02628](#), [doi:10.1007/JHEP01\(2019\)015](#).
- [33] J. Zaanen, Y.-W. Sun, O. Cubero, K. Schalm, Holographic Duality in Condensed Matter Physics, Cambridge University Press, 2015.
- [34] M. Ammon, J. Erdmenger, Gauge/Gravity Duality: Foundations and Applications, Cambridge University Press, 2015.